http://dx.doi.org/10.12785/ugric/2025015

Instituting Superconducting Qubits for Scientists and Engineers

1st Komail Abdulaziz Radhi
Bahrain Institute for Pearls and Gemstones (DANAT)
Manama, Bahrain
kku.aaziz@gmail.com

2nd Khalil Ebrahim Jasim
Department of Physics, College of Science
University of Bahrain
P.Box 32038, Sakheer, Bahrain
kejasim@uob.edu.bh

***Abstract*—In the last two decades, a spectacular development in the superconducting qubits has been accomplished experimentally as well as theoretically. The main reason for that is the realization that superconducting qubits can play a crucial role in the emergent field of quantum information processing and quantum computing. The interaction of superconducting qubits with the quantized electromagnetic field leads to make the circuit quantum electrodynamics, inspired by cavity quantum electrodynamics. The field of superconducting qubits and circuit QED is fast growing and branching to diverse applications in multidisciplinary fields. This makes it harder for first-time readers to follow-up. Therefore, this article is targeting to introduce in an intuitive way the topic of superconducting qubit and circuit QED by giving all the mathematical background, Lagrangian formalism for electric circuits, interaction Hamiltonian, and contextual physical interpretation essential to anew scientists and engineers planning to be specialized in this field as well as portraying a wide vantage for higher studies through the suggested recommendation resulted from the simulated examples and written code based on Python packages and Qiskit software. In this article, the superconducting qubits, transmon and fluxonium, are reviewed after introducing the abstract definition of a quantum bit. Moreover, light-matter interaction in fluxonium qubit and quantization of transmission line resonator are discussed briefly. Some of the simulated systems such as the energy levels of fluxonium as a function of offset flux are presented. Finally, applications of superconducting qubits in quantum computing and other fields such as quantum transistors, quantum machines and metamaterials are discussed.**

***Index Terms*—Superconducting qubits, circuit QED, quantum logic gate, fluxonium, transmon.**

I. Introduction

Quantum computing is about to revolutionize the technology we have today. The aim of this article is to draw the roadmap of quantum computing. Starting from the history of implementing quantum systems to do computing, going through the abstract definition of qubits as information units. Embracing the physical realizations of qubits and explaining the importance and novelty of superconducting qubits as a realization of qubits and as an important field of physics that has applications in science and engineering.

In section I, we briefly review the history behind the idea of quantum computing, then followed by laying the foundations of the abstract definition of qubit. In section II, we state what the qubits physically are and why choosing superconducting qubits among the others. The mathematical tools and the physical models for studying superconducting qubits are discussed in detail in section III. Section IV reviews the fundamental and most well-known superconducting qubit models by explaining their circuit design and their energies. In section V, circuit QED is introduced and how this field represents the light-matter interaction in superconducting qubits. Lastly, section VI, discusses the applications of superconducting qubits in the computing thoroughly and other scientific applications briefly.

A. Historical Review

In 1980s, the American theoretical physicist, Richard Feynman, introduced the idea of quantum computing in his lectures ”Potential advantages of computing with quantum systems”. Few years later, the British physicist, David Deutsch, proposed the idea of a universal quantum computer [1]. After that, several contributions developed quantum algorithms that tackle issues like factorization [2, 3], searching in databases [4] and simulations. However, quantum computers aim to overcome the classical computers reaching the quantum supremacy.

B. From Classical Bit to Quantum Bit

Let's start first by defining the so-called term *bit*. The *b*inary dig*it*, or *bit*, is defined as the smallest unit of classical information. That means it quantifies the information capacity of a two-level system [5]. Abstractly speaking, any thing with two distinct values could be represented logically as a classical bit (e.g., coins (head/tails), electric switch (on/off), etc.).

The bits are used to store the encoded information, manipulating these bits is done by *logic gates*. By logic gates, all computations are performed. There are single-bit gates (e.g. NOT gate) and two-bit gates (e.g. AND gate, OR gate, XOR gate, etc.) that can take 2 input bits and give 1 output bit; see Fig. 1a. The gates NOT, AND, OR perform a universal gate set[1].

We have explained earlier what the bits are and how to manipulate them with logic gates. But what are these gates? One of the easiest ways to enact them is by electric circuits. If we represent the bit by a light bulb, it could be either on or off, the gates could be represented by mechanical switches. Fig. 1b and 1c show the electrical circuit representation of

[1] A *universal gate set* is a set of gates that span all possible logic operations in the truth table. It is one of the requirements to make a quantum computer, see subsection VI-A1.

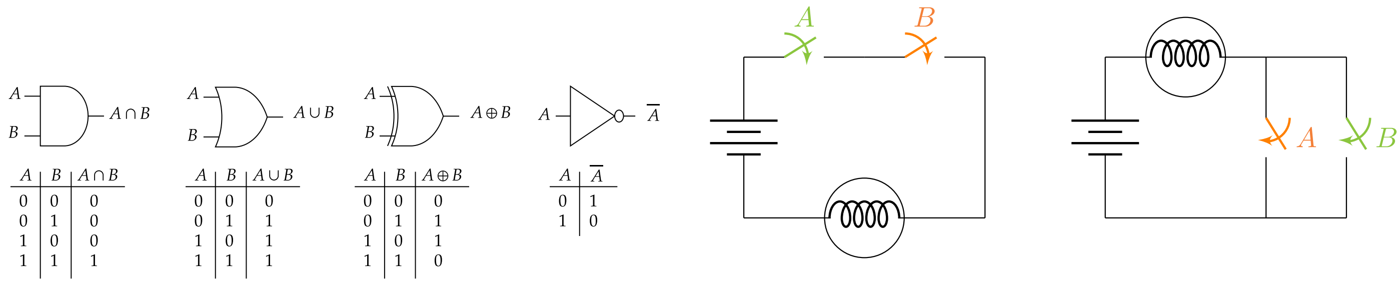

(a) Logic gates (b) AND gate (c) OR gate

Fig. 1: (a) Logic gates and their truth table (From left to right, the gates are: AND, OR, XOR and NOT. You can see that NOT is a single-bit gate and the rest are two-bits gates). The circuit representation of (b) AND (c) OR logic gates.

AND and OR gates. These are very simple examples of realizations of logic gates for the sake of explaining the principle. Nevertheless, more complicated realizations are used in daily life such as transistor or diode logic gates.

The quantum bit or *qubit* is similar to the classical bit that it has two values, either 0 or 1. But in contrast to classical bits, qubits inherit quantum-mechanical properties such as superposition and entanglement.

Superposition: The state of the qubit 0 and 1 are represented in Dirac notation (bra-ket notation) as: $|1\rangle$ and $|0\rangle$, or their superposition:

$$|\psi\rangle = \alpha|0\rangle + \beta|1\rangle \tag{1}$$

Where $\alpha, \beta \in \mathbb{C}$. After the qubit is measured, the probability to be in the $|0\rangle$ state is $|\alpha|^2$ and $|\beta|^2$ for state $|1\rangle$. The sum of the probabilities should equal to 1:

$$|\alpha|^2 + |\beta|^2 = 1 \tag{2}$$

These states - $|0\rangle$ and $|1\rangle$ - can be represented as the poles of sphere called *Bloch sphere*. Bloch sphere is a sphere with unitary radius and states $|0\rangle$ and $|1\rangle$ as north and south poles, respectively. The advantage of Bloch sphere is that it can always represent the qubit's state, i.e. any point on the sphere could represent a valid superposition state of the qubit.

Entanglement: When dealing with multiple qubits, a quantum mechanical property could be exploited, that cannot be done on classical bits, it is *entanglement*. To say, entanglement means that the state of a qubit is not independent of the other entangled qubit. Let us define entangled states using the bra-ket notation. When we have multiple qubits, each of them has its own states, their state together are the tensor product of them:

$$|\psi_1\rangle \otimes |\psi_2\rangle \tag{3}$$

For example, if $|\psi_1\rangle = |0\rangle$ and $|\psi_2\rangle = |1\rangle$, then their tensor product, in a compressed form, is $|01\rangle$. Let us do another example, if:

$$|\psi_1\rangle = \frac{1}{2}(|0\rangle + \sqrt{3}\,|1\rangle), \qquad |\psi_2\rangle = \frac{1}{\sqrt{2}}(|0\rangle - |1\rangle)$$

Then their tensor product is:

$$|\psi_1\rangle \otimes |\psi_2\rangle = \frac{1}{2\sqrt{2}}(|00\rangle - |01\rangle + \sqrt{3}\,|10\rangle - \sqrt{3}\,|11\rangle) \tag{4}$$

One important thing on this product is that we can write it back as a tensor product of two qubits, i.e. factorizing it. The states of multiple qubits that cannot be factorized are the *entangled states*. Here are some states that cannot be factorized, implied that they are entangled:

$$|\Phi^+\rangle = \frac{1}{\sqrt{2}}(|00\rangle + |11\rangle) \tag{5}$$

$$|\Phi^-\rangle = \frac{1}{\sqrt{2}}(|00\rangle - |11\rangle) \tag{6}$$

$$|\Psi^+\rangle = \frac{1}{\sqrt{2}}(|01\rangle + |10\rangle) \tag{7}$$

$$|\Psi^-\rangle = \frac{1}{\sqrt{2}}(|01\rangle - |10\rangle) \tag{8}$$

These are the so-called *Bell states*. In subsection VI-A2, we are going to show an example of how to create entanglement using quantum logic gates.

However, if we perform measurement on a single qubit in a product state, it does not perturb the state of the other qubit. For example, if we perform measurement on $|\psi_1\rangle$, we get 25% for being in state $|0\rangle$ and 75% for being in state $|1\rangle$. So, if we measure $|\psi_1\rangle$ in the product state (4), we get:

$$\left|\frac{1}{2\sqrt{2}}\right|^2 + \left|\frac{-1}{2\sqrt{2}}\right|^2 = \frac{1}{8} + \frac{1}{8} = 0.25$$

$$\left|\frac{\sqrt{3}}{2\sqrt{2}}\right|^2 + \left|\frac{-\sqrt{3}}{2\sqrt{2}}\right|^2 = \frac{3}{8} + \frac{3}{8} = 0.75$$

Which is the same result. As mentioned earlier, the entangled states are not independent of each other. So, if we measure a single qubit in entangled state with another qubit, for sure, it would affect the state of the latter qubit. Meaning that you can tell what is the state of the second qubit based on the state of the first qubit. In state $|\Phi^+\rangle$ if we perform measurement on the left qubit, it has 50-50 probability of being in state $|0\rangle$ or $|1\rangle$. After measurement, if the left qubit is found in state $|0\rangle$ it directly implies that the right qubit is definitely in state $|0\rangle$. This entangled state is called *maximally entangled state*. The Bell states are maximally entangled states.

If a measurement is performed on a qubit in an entangled state with other qubits, and does not determine the state of other qubits. Meaning that you can not tell the state of the second qubit definitely based on the state of the first qubit. This entangled state is called *partially entangled state*.

II. Physical Realization of Qubits

The abstract definition of the qubit as an information bit is explained. Next, the physical realization of qubits. Here, physical realization means the actual implementation of the abstract definition. So, physical realization of qubit means the qubit in real life not abstraction.

Many companies invest in quantum computing and implement different realizations of superconducting qubits; for example, IonQ with trapped ions [6], Intel with superconducting and semiconductor spin qubits [7]. But most of the companies are developing and investing in superconducting qubits such as IBM [8], Google [9], and Amazon [10].

A. Other physical realization of qubits

To realize a physical qubit, any quantum system with two distinct states, or that could be treated in certain conditions as a two-level system, can be used as a qubit. There are different examples that are investigated and explored for this purpose: Photons, trapped ions, cold atoms, nucleus spin by nuclear magnetic resonance (NMR), quantum dots, solid-state qubits, and last but not least, superconducting qubits. The aforementioned examples are not an exhaustive list, as there are additional unique qubit realizations currently under investigation.

Here are some physical qubits, that have been developed in the last two decades in more details:

Photons: The polarization state of the photon is a two-level system. It is either horizontally, vertically polarized or the superposition between them. Manipulating and controlling the photons is done by using linear and nonlinear optical components. The field of controlling the state of photons is called *Integrated Quantum Photonics*, see [11].

Trapped Ions: Trapped-ion qubits exploit the energy levels of trapped ions in radio frequency traps. Trapped-ion qubits are one of the promising qubits that meet DiVincenzo criteria, see subsection VI-A1.

Quantum Dots: The spin of electrons that are confined in the quantum dot is considered as a qubit. Because the electron's spin have two distinct value; either $1/2$ or $-1/2$.

B. Choosing superconducting qubits in this article

Superconducting qubits are chosen in this article for several reasons. However, a common point between defining the binary states of trapped-ion qubits and superconducting qubits that are both based on choosing two-energy levels and ignoring all other levels. Although, a major difference between superconducting qubits and all other physical realizations is their quantum behavior.

Quantum phenomena are found in *micro*scopic particles (e.g., atoms, electrons, etc.). Occasionally, it is not practical to use small particles as physical qubits. In contrast to the previous physical qubits, the superconducting qubits have a *macro*scopic quantum system, instead of microscopic. And a quantum behavior on a macroscopic scale would be much preferred. Because superconductors could maintain macroscopic quantum behavior, this opens a new area to study superconductivity in the field of qubits and quantum computing.

In addition to the macroscopic quantum behavior, superconducting qubits have higher designability than others. This will be clear when representing different designs of superconducting qubits in section IV. Also, they are easy to couple and to control by microwaves. Moreover, they are more scalable than others.

III. Circuit Representation

Earlier in the previous sections, we have explained what is the abstract definition of the qubit and how it represents the binary data differently from classical bits by utilizing the quantum mechanical behavior of the system. Then, the realization of the qubit can be done using different quantum systems. However, the realizations (other than superconducting qubits) have "relatively" clearer way of representing the binary levels of the qubit (e.g. photon spin). But in superconducting qubits are not that straightforward. In order to establish the two-level system of superconducting qubits, we have to establish a physical model to study them. Equivalent circuit model[2] is an ideal representation of the electrical properties of superconductors.

The different types of superconducting qubits, explained in section IV, have different circuit models. From these models, we can study the properties of the qubit and define the binary levels. In order to define the binary levels of the superconducting qubit, we have to establish a mathematical method to study the electrical circuit.

Lastly, modeling the superconducting qubits by their equivalent circuit model inherit their classical behavior (i.e. the continuity of variables). This requires promoting from the classical model to the quantum model, in subsection III-B. Then, the system can be studied using the quantum mechanics tools, and the binary levels are defined.

[2]Here it is called *modeling* because the superconductors are not designed as electrical components. Instead, they are superconducting sheets, or islands, that exhibit electrical properties best represented by circuit elements.

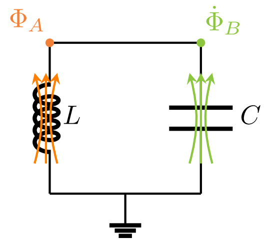

Fig. 2: LC oscillator.

A. Lagrangian formalism

Before delving into modeling the qubits using their equivalent circuits, we must lay the foundation for a proper approach to studying electrical circuits. This concern arises because the normal way of dealing with electrical circuits will not be suitable for our purposes. The normal methods of analyzing circuits, such as Kirchhoff's rules or any other methods from circuit analysis textbooks, are not wise choices. The most important physical quantity to deal with in quantum mechanics is energy. The variables of interest are not currents or voltages[3]. For this reason, it is necessary to deal with these circuit models in a different way.

Here, the Lagrangian formalism comes into action. It allows us to deal with our systems directly by energy, and then from studying these energies we can derive any equation in the system. For example, the trajectory of a projectile can be derived from Newton's equations, which they depend on forces and accelerations. We can derive the same trajectory of the projectile by using Lagrangian mechanics, which deals with energies. Similarly for electrical circuits, by using Lagrangian formalism to deal with the circuit components by their energies. By this method, the Lagrangian is defined for the model. Then, the Hamiltonian is derived from the Lagrangian which will be quantum mechanically quantized later on.

1) LC Oscillator: The superconducting quantum circuits are different in size and complexity. To start with, the LC oscillator, is the simplest and the most important superconducting circuit model to start with and to use Lagrangian formalism on. We will go through the Lagrangian formalism step by step, then the same method can be applied with slight modifications to different superconducting circuits. Before starting, choosing the LC oscillator and not any other electrical circuit is because of its property of conserving energy and oscillating it between inductive and capacitive components. Also, the quantum-promoted LC oscillator behaves exactly the same as the quantum harmonic oscillator which is an important quantum system that is used in many quantum applications and as an approximation for complex quantum systems. Not to forget, LC oscillators are also used as single-mode resonators to couple qubits, see section V.

[3]Of course, they are important, but they are not the proper variables to deal with quantum mechanically

Consider the LC oscillator shown in Fig. 2. Let us breakdown the energy terms in the circuit, we have two energies: Inductive and capacitive energy. To use the Lagrangian formalism, the energies should be defined as kinetic and potential energy. Here, we will define the kinetic energy and potential energy as follows[4]:

$$T = \frac{1}{2}LI^2 \qquad U = \frac{1}{2C}Q^2$$

Then the Lagrangian is:

$$\mathcal{L} = T - U = \frac{1}{2}LI^2 - \frac{1}{2C}Q^2 \tag{9}$$

Writing I as $\dot{Q}$ makes intuition about the relation of inductive and capacitive energies with mechanical kinetic and potential energy:

$$\mathcal{L} = \frac{1}{2}L\dot{Q}^2 - \frac{1}{2C}Q^2 \tag{10}$$

However, the assumption of which term is kinetic energy and which is potential energy means choosing what is your dynamical variable. Choosing the capacitive energy as the potential energy means that the charge Q is the dynamical variable, and the Lagrangian is a function of Q and $\dot{Q}$, i.e., $\mathcal{L}(Q, \dot{Q})$. Similarly, when choosing the inductive energy as the potential energy, the flux Φ is our dynamical variable, and the Lagrangian is $\mathcal{L}(\Phi, \dot{\Phi})$.

In our notation, we choose to use $\mathcal{L}(\Phi, \dot{\Phi})$ and the dynamical variable is the flux Φ. So, the Lagrangian now is:

$$\mathcal{L} = \frac{1}{2}C\dot{\Phi}^2 - \frac{1}{2L}\Phi^2 \tag{11}$$

Here $Q = C\dot{\Phi}$ and $\Phi = LI$. However, Lagrangian formalism is an equivalent way to Kirchhoff's rules in analyzing circuits. Each method can be used, but one could be a wiser choice than the other (see Appendix B).

B. Circuit Quantization

The Lagrangian of the LC oscillator is derived and ready to be used. In quantum mechanics, we do not use the Lagrangian of the system. Instead, we use the Hamiltonian of the system[5].

Taking the Lagrangian $\mathcal{L}(\Phi, \dot{\Phi})$ from (11), we could apply Legendre transformation [12] on the Lagrangian of LC oscillator, taking the flux Φ as the coordinate and the charge Q as the momentum conjugate, to obtain the Hamiltonian:

$$\mathcal{H}_{LC} = Q\dot{\Phi} - \mathcal{L} = \frac{1}{2C}Q^2 + \frac{1}{2L}\Phi^2 \tag{12}$$

Here $\dot{\Phi} = Q/C$. The resonance frequency of the LC oscillator is $\omega_r = 1/\sqrt{LC}$. By implementing this in the Hamiltonian (12):

$$\mathcal{H}_{LC} = Q\dot{\Phi} - \mathcal{L} = \frac{1}{2C}Q^2 + \frac{1}{2}C\omega_r^2\Phi^2 \tag{13}$$

[4]It does not matter what to choose as kinetic energy or potential energy. Both choices are equivalent to each other and give the same behavior.

[5]The Hamiltonian represents the total energy of the system, while the Lagrangian not. It is a quantity that represents the difference between the kinetic and the potential energy

This draws the analogy between the mechanical harmonic oscillator (e.g. a mass attached to a spring) and LC oscillator, where the flux Φ is the position variable of the oscillator, and Q is the momentum conjugate with mass C and spring constant $1/L$.

By promoting the charge and flux variables to non-commuting operators using the canonical quantization:

$$\left[\hat{\Phi}, \hat{Q}\right] = i\hbar \tag{14}$$

Thus, the Hamiltonian operator would be analogous to the Hamiltonian of quantum harmonic oscillator:

$$\hat{\mathcal{H}}_{LC} = \frac{1}{2C}\hat{Q}^2 + \frac{1}{2}C\omega_r^2\hat{\Phi}^2 \tag{15}$$

Ladder operators are beneficial algebraic tools in quantum mechanics to solve Schrödinger equation and determine the energy levels of the system. Drawing the analogy between the quantum harmonic oscillator and the LC oscillator[6], where $m \to C$, $\hat{x} \to \hat{\Phi}$ and $\hat{p} \to \hat{Q}$. Then the ladder operators would be:

$$\hat{a}^\dagger = \frac{1}{\sqrt{2\hbar\omega_r C}}\left(C\omega_r\hat{\Phi} + i\hat{Q}\right) \tag{16}$$

$$\hat{a} = \frac{1}{\sqrt{2\hbar\omega_r C}}\left(C\omega_r\hat{\Phi} - i\hat{Q}\right) \tag{17}$$

Where $\hat{a}^\dagger$ and $\hat{a}$ are the creation and annihilation operators, respectively. Here, the creation operator $\hat{a}^\dagger$ creates a photon of frequency ω_r stored in the circuit. By simple arithmetic, the flux and charge operators can be written in terms of ladder operators as follows:

$$\hat{\Phi} = \Phi_{ZPF}\left(\hat{a}^\dagger + \hat{a}\right) \tag{18}$$

$$\hat{Q} = iQ_{ZPF}\left(\hat{a}^\dagger - \hat{a}\right) \tag{19}$$

Here $\Phi_{ZPF} = \sqrt{\hbar/2C\omega_r}$ and $Q_{ZPF} = \sqrt{\hbar C\omega_r/2}$. Here, ZPF means zero-point fluctuations. That is the standard deviation of the flux or charge operators (i.e. Φ_{ZPF} or Q_{ZPF}). The zero-point fluctuation values give us insights on the fluctuations of the electric charge and magnetic flux.

By substituting the flux and charge operators to rewrite the Hamiltonian in ladder operators, we get:

$$\hat{\mathcal{H}}_{LC} = \hbar\omega_r\left(\hat{a}^\dagger\hat{a} + \frac{1}{2}\right) \tag{20}$$

In (20) the factor $\hbar\omega_r$ has the dimensions of energy, and the term $\hat{a}^\dagger\hat{a}$ gives the number of the energy state of the system. From this, the energy levels are equidistant from each other by $\hbar\omega_r$. So, this proves that the LC oscillator behaves the same as the quantum harmonic oscillator.

The equidistant energy levels are the result of the linear inductive behavior of the LC oscillator. That makes the LC oscillator a bad choice as a circuit model for qubits, but useful as a single-mode resonator. This harmonicity should be broken to have non-equidistant energy levels, see subsection III-D.

[6]It can be derived solely without using the analogous example of quantum harmonic oscillator. See [13] for the algebraic way of deriving ladder operators, section 2.3.1

C. Reduced operators

The ladder operators, in opposite to the flux and charge operators, are dimensionless operators. Dealing with dimensionless operators has benefits in order to ease the calculations and decrease the number of factors to control. For this reason, the flux and charge operators will be reduced to dimensionless operators.

In superconductors, the charge is quantized in terms of pairs of electrons called Cooper pairs, see Appendix A. So, the charge operator will be reduced to:

$$\hat{n} \equiv \frac{\hat{Q}}{2e} \tag{21}$$

This is the charge number operator, which represents the number of Cooper pairs, and it is a discrete operator. Next we have:

$$\hat{\varphi} \equiv \frac{2\pi}{\phi_0}\hat{\Phi} \tag{22}$$

This is the reduced flux operator or phase operator and it is a compact operator (i.e. periodic). It's called *phase operator* because it represents the phase of the macroscopic wavefunction on a superconductor island. And ϕ_0 is the quanta of magnetic flux and called *fluxon*, and it is equal to $h/2e \approx 2.067834 \times 10^{-15}Wb$.

Substituting back in the canonical quantization:

$$\left[\frac{\phi_0}{2\pi}\hat{\varphi}, 2e\hat{n}\right] = i\hbar$$
$$\Rightarrow [\hat{\varphi}, \hat{n}] = i \tag{23}$$

This commutation relation obviously shows the dimensionless nature of the reduced operators. Another important relation to derive, is the Heisenberg uncertainty principle of the reduced operators. It could be derived using the generalized uncertainty principle, as explained in [13]. Thus, the relation will be:

$$\Delta\varphi\Delta n \geq \frac{1}{2} \tag{24}$$

1) LC oscillator: We will start to examine the reduced operators on the LC oscillator. Let us substitute the reduced operators in the Hamiltonian (15):

$$\hat{\mathcal{H}}_{LC} = \frac{1}{2C}(2e\hat{n})^2 + \frac{1}{2}C\left(\frac{1}{LC}\right)^2\left(\frac{2\pi}{\phi_0}\hat{\varphi}\right)^2$$
$$\Rightarrow \hat{\mathcal{H}}_{LC} = 4E_C\hat{n}^2 + \frac{1}{2}E_L\hat{\varphi}^2 \tag{25}$$

Where $E_C = e^2/2C$ and $E_L = (\phi_0/2\pi)^2/L$ are the capacitive and inductive energy, respectively. This brings intuition about how the dominant energy term affecting the behavior of the system. These energy factors will assist in defining the working regime for each qubit as shall be seen later.

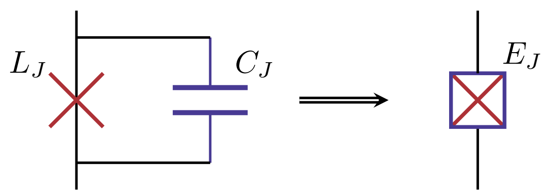

Fig. 3: The electric symbol for Josephson junction.

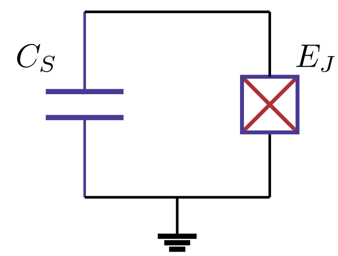

Fig. 4: Transmon qubit.

D. *Josephson junction*

Josephson effect is a macroscopic quantum phenomenon happens when two superconductors are placed in proximity with some barrier between them, see Appendix A. The device that utilizes Josephson effect is called a *Josephson junction*. The Josephson junction exhibits a nonlinear inductive behavior as a function of the magnetic flux. It is defined as follows:

$$L_J(\Phi) = \frac{\phi_0}{2\pi I_c}\frac{1}{\cos(2\pi\Phi/\phi_0)} \tag{26}$$

where I_c is the critical current. Due to the proximity of the superconductors, there is an intrinsic capacitance between the two islands. In circuit representation, the Josephson junction is represented by an "X" symbol (for the nonlinear inductance) inscribed inside a square (represent the intrinsic capacitance), see Fig. 3.

Josephson junction is an essential element in qubits. In order to use it in analyzing the qubits. We need to find the energy stored in the Josephson inductance. To do that, we need to use both Josephson DC and AC effects, see Appendix A, as follows:

$$\begin{aligned} E &= \int V(t)I(t)\,dt \\ &= \int \frac{d\Phi(t)}{dt} I(t)\,dt \\ &= \int \frac{d\Phi(t)}{dt}\left(I_c \sin\left(\frac{2\pi}{\phi_0}\Phi\right)\right) dt \\ &= -\frac{\phi_0 I_c}{2\pi}\cos\left(\frac{2\pi}{\phi_0}\Phi\right) \end{aligned}$$

By writing the energy in terms of reduced quantized phase variable:

$$E = -E_J \cos\hat{\varphi} \tag{27}$$

Where $E_J = \phi_0 I_c/2\pi$. This quantity is proportional to the rate of tunneling of Cooper pairs through the insulator layer, which is actually because of the current I_c.

This nonlinearity of Josephson junction inductance plays a crucial role in providing the necessary anharmonicity in superconducting qubits. Making the anharmonic energy levels to the qubits, i.e. the energy levels are not equidistant. The anharmonicity of qubits is a necessary condition to provide a functional qubit, but not sufficient. Other criteria must be there to have fully-functioning qubit, see subsection VI-A1.

IV. Superconducting Qubits

Current models and designs of superconducting qubits are derived from 3 basic types of qubits [14, 15]: charge-based qubits, flux-based qubits, and phase-based qubits. These 3 types are classified by the ratio of capacitive energy to Josephson energy (i.e. E_J/E_C). As mentioned in section III, reduced operators, the charge number operator $\hat{n}$ and the phase operator $\hat{\varphi}$ are canonically conjugate and they obey Heisenberg uncertainty principle. So when the capacitive term dominates, the phase operator has larger quantum fluctuations than charge number operator, and vice versa. Basically, the basic design of charge-based qubits depends on the charge number operator $\hat{n}$ and flux-based qubits depend on the phase operator $\hat{\varphi}$. In this section, we will go through the charge- and flux-based qubits to introduce the transmon and fluxonium qubits.

A. *Charge-based qubits*

1) Cooper Pair Box: The Cooper pair box (CPB) is the first version of charge-based superconducting qubit. It is formed by connecting two superconducting islands by an insulator, this is a Josephson junction, see Appendix A. Cooper electron pairs tunnel from the first island, called the *electrode*, toward the second island, called the *reservoir*, through the insulator junction. The Hamiltonian of CPB is:

$$\hat{\mathcal{H}}_{CPB} = 4E_C(\hat{n} + n_g)^2 - E_J \cos\hat{\varphi} \tag{28}$$

Here $E_C = e^2/2(C_J + C_g)$. The n_g is the gate charge number caused by coupling the Josephson junction to the gate capacitor, C_g. It is a continuous variable in contrast to the charge number operator $\hat{n}$ which is discrete.

2) Transmon: Cooper pair boxes are sensitive to the gate charge caused by the gate capacitance, and that affects the energy levels. Hence the transmon qubit is introduced by [16] to solve this issue and create a more stable energy levels with less charge sensitivity. The transmon is a Josephson junction, smaller compared to the Cooper pair box but shunted with a large capacitance C_S to decrease the capacitance energy E_C

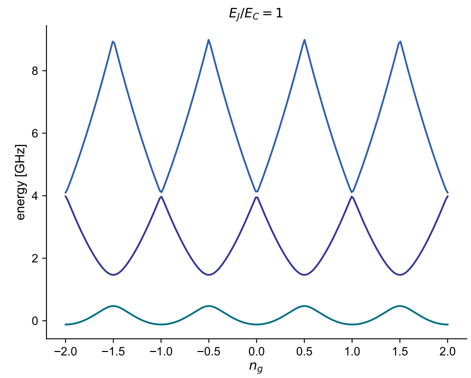

(a) $E_J/E_C = 1$

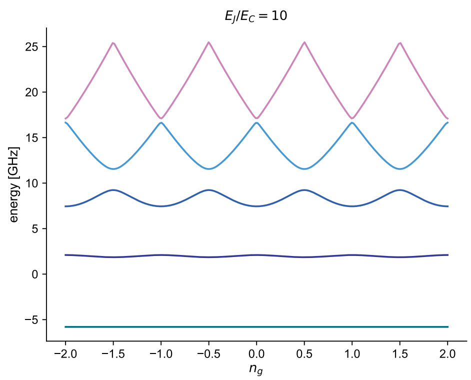

(b) $E_J/E_C = 10$

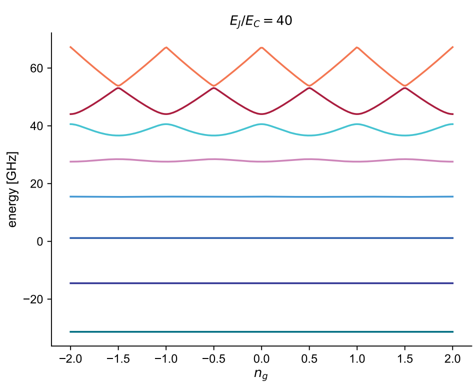

(c) $E_J/E_C = 40$

Fig. 5: Charge insensitivity of transmon qubit. The larger the value of E_J/E_C the more the energy levels are stable and insensitive to gate charge. Also, the sensitivity to gate charge is inevitable in higher energy levels, but in qubits our concern is on the first two levels.

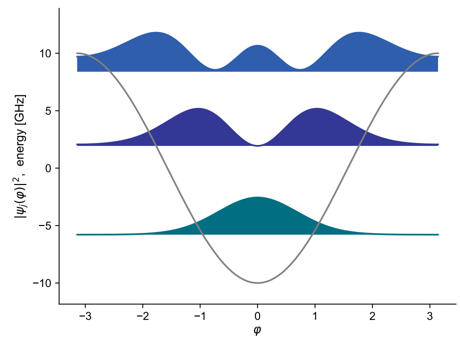

(a) $E_J/E_C = 10$

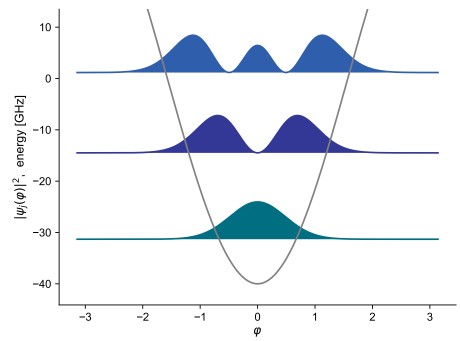

(b) $E_J/E_C = 40$

Fig. 6: The wavefunctions in base φ for two transmon qubits with two E_J/E_C ratios. The larger the value of E_J/E_C the more valid the approximation in (30) is.

and by increasing the gate capacitance C_g, as well, see Fig. 4. So, the dominant term will be the flux term, which will have less quantum fluctuations. That makes the dominant variable is the flux Φ.

Since the transmon qubit is insensitive to the offset charge in their operating regime (i.e. large E_J/E_C), see Fig. 5, then we can write the transmon Hamiltonian as:

$$\hat{\mathcal{H}}_T = 4E_C\hat{n}^2 - E_J\cos\hat{\varphi} \tag{29}$$

Here is the capacitance energy $E_C = e^2/2(C_J + C_g + C_S)$. And the transmon qubit is represented in a superconducting circuit as shown in Fig. 4.

By approximating the Josephson junction energy term in the Hamiltonian, by expanding the cosine to:

$$\cos\hat{\varphi} = 1 - \frac{\hat{\varphi}^2}{2!} + \frac{\hat{\varphi}^4}{4!} + \dots$$

Thus, the transmon Hamiltonian, up to the first nonlinear term, would be:

$$\hat{\mathcal{H}}_T = 4E_C\hat{n}^2 + \frac{1}{2}E_J\hat{\varphi}^2 - \frac{1}{4!}E_J\hat{\varphi}^4 \tag{30}$$

Notice here the constant term is dropped because it is a constant perturbation and just shifts the whole spectrum by constant amount, i.e. $-E_J$.

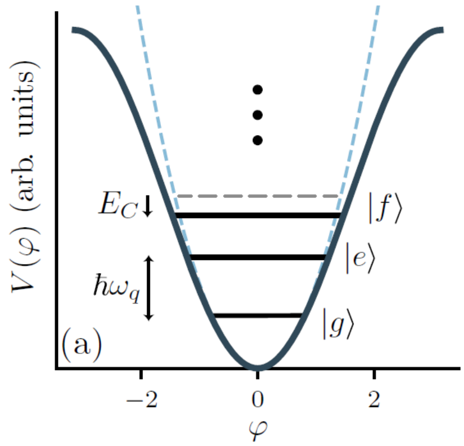

Fig. 7: The anharmonicity of transmon qubit potential well compared to the harmonic oscillator (dashed blue). Figure is adapted from [17].

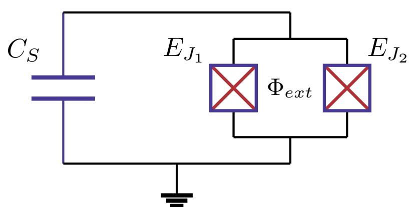

Fig. 8: Flux-tunable transmon.

Defining the ladder operators based on the linear terms (the first two terms) in the transmon Hamiltonian (30), and writing the reduced operators in terms of them:

$$\hat{\varphi} = \frac{1}{\sqrt{2}}\left(\frac{8E_C}{E_J}\right)^{1/4}\left(\hat{b}^\dagger + \hat{b}\right) \tag{31}$$

$$\hat{n} = \frac{i}{\sqrt{2}}\left(\frac{E_J}{8E_C}\right)^{1/4}\left(\hat{b}^\dagger - \hat{b}\right) \tag{32}$$

Where $\hat{b}$ and $\hat{b}^\dagger$ are the annihilation and creation operators, respectively. Then the transmon Hamiltonian in ladder operators is:

$$\hat{\mathcal{H}}_T = \sqrt{8E_C E_J}\left(\hat{b}^\dagger\hat{b} + \frac{1}{2}\right) - \frac{E_C}{12}\left(\hat{b}^\dagger + \hat{b}\right)^4 \tag{33}$$

Fig. 6 (as depicted on the previous page) shows the energy levels and wavefunctions of two transmon qubits with different E_J/E_C ratios. Notice that the shape of the potential well shows the validity of the approximation in (30), which is valid for the transmon regime.

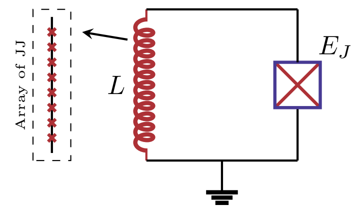

Fig. 9: Fluxonium circuit with array of JJ.

Anharmonicity of Transmon: The anharmonic nature of the qubit is a vital issue, because the energy spacing is different for each transition between energy levels. If the energy spacing is identical for all levels, that means the transitions between the energy levels would not be distinguishable.

Here in transmon qubit, to show the anharmonicity, the rotation-wave approximation is applied on the power 4 term [17], then the approximated Hamiltonian is:

$$\hat{\mathcal{H}}_T = \left(\sqrt{8E_C E_J} - E_C\right)\left(\hat{b}^\dagger\hat{b} + \frac{1}{2}\right) - \frac{E_C}{2}\hat{b}^\dagger\hat{b}^\dagger\hat{b}\hat{b} \tag{34}$$

Fig. 7 shows the anharmonicity of the transmon qubits compared to the LC oscillator, in other words, the quantum harmonic oscillator.

Flux-tunable Transmon: The transmon qubit has a fixed operating frequency. There is the flux-tunable transmon qubit, where the frequency of this qubit is tuned by the applied external flux. Here, the Josephson junction in transmon qubit, is replaced by a superconducting quantum interference device (SQUID). Then the Hamiltonian is:

$$\hat{\mathcal{H}}_T = 4E_C\hat{n}^2 - E_{J1}\cos\hat{\varphi}_1 - E_{J2}\cos\hat{\varphi}_2 \tag{35}$$

Here we have two terms for the Josephson junction, because the SQUID consists of two Josephson junctions, see Fig. 8.

B. *Flux-based qubits*

1) Fluxonium: The fluxonium is constructed by shunting an array of small Josephson junctions to a large Josephson junction to obtain a large shunted inductance to the Josephson junction, see Fig. 9.

This is done to make the qubit less sensitive to the offset flux noise, similar to the motivation for the transmon qubit to charge noise. The inductive noise comes from the large shunted inductance that is in proximity to another inductor with a DC current flowing through making an offset flux. So the Hamiltonian can be written as:

$$\begin{aligned}\hat{\mathcal{H}}_{Fluxonium} = 4E_C(\hat{n} + n_g)^2 - E_J\cos\hat{\varphi} \\ + \frac{1}{2}E_L(\hat{\varphi} + \varphi_g)^2\end{aligned} \tag{36}$$

Where $E_L = (\phi_0/2\pi)^2/L$, which is the inductive energy of the large inductance. It is convenient to perform unitary transformations [13] on the operators $\hat{n}$ and $\hat{\varphi}$. The unitary

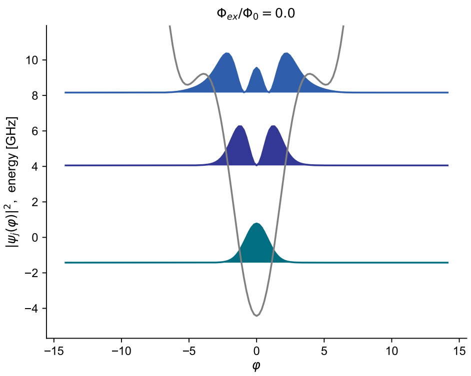

(a) $\varphi_g/2\pi = 0$

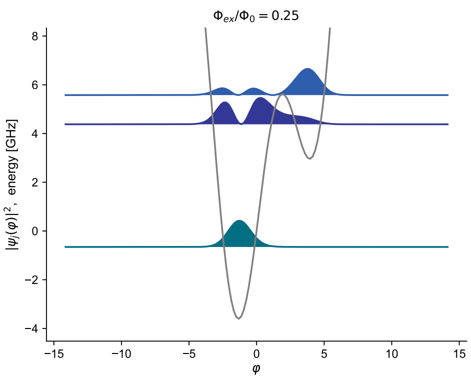

(b) $\varphi_g/2\pi = 0.25$

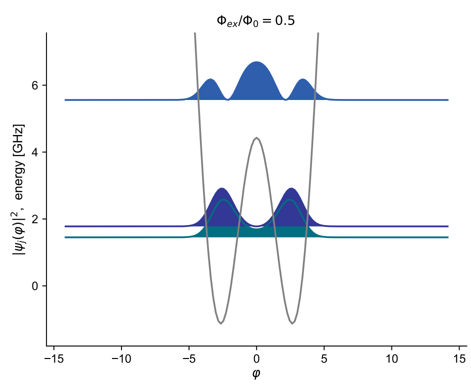

(c) $\varphi_g/2\pi = 0.5$

Fig. 10: The wavefunctions in base φ for 3 fluxonium qubits with different offset flux φ_g. The double well shape changes depending on the value of the offset flux. The energy levels of the wavefunctions changes with the offset flux.

transformation is done to get rid off the offset charge and flux as:

$$\hat{U} = e^{i\hat{\varphi}n_g} e^{i\varphi_g \hat{n}} \tag{37}$$

Where this transformation when operates on $\hat{n}$ and $\hat{\varphi}$ yields:

$$\hat{U}\hat{n}\hat{U}^{\dagger} = \hat{n} - n_g \tag{38}$$

$$\hat{U}\hat{\varphi}\hat{U}^{\dagger} = \hat{\varphi} - \varphi_g \tag{39}$$

Then the Hamiltonian would be:

$$\hat{\mathcal{H}}_{Fluxonium} = 4E_C\hat{n}^2 + \frac{1}{2}E_L\hat{\varphi}^2 - E_J\cos\left(\hat{\varphi} - \varphi_g\right) \tag{40}$$

Here we cannot approximate the cosine term as in (30), because the ratio E_J/E_C is not as large as in the transmon qubit. So, it must be kept as it is. Now, the potential well is not a quadratic well. Instead, it is quadratic + cosine, and it depends on the offset flux. Fig. 10 shows the wavefunctions of the first 3 energy levels for different offset fluxes. It is clear that the energy levels are influenced by the offset flux by noticing the energy difference between the first 3 energy levels in Fig. 10.

Now, by introducing the ladder operators for the fluxonium qubit[7] in a similar way to transmon qubit:

$$\hat{\varphi} = \frac{1}{\sqrt{2}}\left(\frac{8E_C}{E_L}\right)^{1/4}\left(\hat{b}^{\dagger} + \hat{b}\right) \tag{41}$$

$$\hat{n} = \frac{i}{\sqrt{2}}\left(\frac{E_L}{8E_C}\right)^{1/4}\left(\hat{b}^{\dagger} - \hat{b}\right) \tag{42}$$

C. State-of-art Qubits

Among the years different designs of superconducting qubits were developed in the field of superconductor qubits, such as: Unimon [18], $\cos(2\phi)$ qubit [19], Blochnium [20], Bifluxon qubit [21] and plasmonium qubit [22]. Each of them has its unique circuit representation, refer to the references for more details.

V. Circuit QED

A. circuit QED vs. cavity QED

To briefly compare between cavity QED and circuit QED, cavity QED studies the atoms or ions coupled to electromagnetic photons inside a resonant cavity. The property of this resonant cavity is that it supports only discrete modes of electromagnetic field. Similarly, circuit QED uses the superconducting qubits as artificial atoms coupled to microwave resonators. Superconducting qubits are called as *artificial atoms* because their energy levels can be changed by manipulating the values of electrical circuit elements. But circuit QED goes further beyond that, because it combines the tools of quantum optics and the physics of superconducting circuits to study more physics fundamentals that cannot be achieved using real atoms.

B. Light-matter Interaction in Fluxonium Qubit

It is inevitable to isolate the qubit from the environment. It should be coupled, intentionally or not, to the environment. To control the qubit and measure it, it should be coupled by a coupling mechanism[8]. In this section, we are coupling the Fluxonium qubit to a coplanar waveguide resonator.

[7]Be careful! They have the same notation for transmon's ladder operator, but they are defined by using E_L instead of E_J.

[8]There are different kind of coupling mechanisms between qubits, see [23]

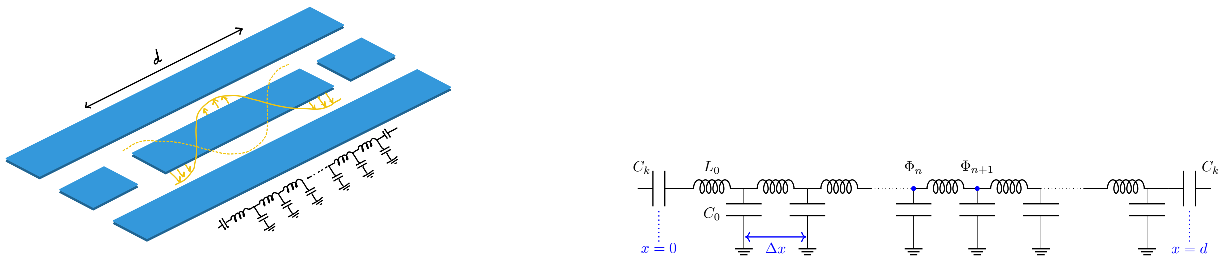

(a) Transmission line (b) Telegrapher Model

Fig. 11: Transmission line resonator and telegrapher model.

Commonly in circuit QED, the electric and magnetic field are confined to 2-dimensional wave guides, called *coplanar waveguide resonator*, see Fig. 11a. This coplanar waveguide resonator acts as a transmission line, and it is modeled by the telegrapher model [24]. Fig. 11b shows the telegrapher model for a 1-dimensional transmission line resonator. Notice that the building blocks of the telegrapher model consist of series inductance L_o represents the self-inductance of the superconductor and shunted capacitance C_o represents the capacitance between the two superconductor substrates and there are no resistive elements because, again, we are dealing with superconducting circuits.

To study the coupling of fluxonium qubit and coplanar waveguide resonator, see Fig. 12a (see the figure on the next page), we have to sum their Hamiltonians. The Hamiltonian of Fluxonium qubit is already derived earlier. Let us derive the Hamiltonian of the resonator[9].

To start with, from the telegrapher model, it has n terms of capacitors and inductors. So, the associated capacitive and inductive energies of the resonator are:

$$T = \frac{Q_n^2}{2C_o} \qquad U = \frac{1}{2L_o}\left(\Phi_{n+1}^2 - \Phi_n^2\right)$$

Notice that, as before, here the coordinate variable is the flux. Also, the nth inductive energy is the flux through joint n, i.e. the difference between the fluxes from the inductors before and after the point. By the same method of deriving the Hamiltonian of LC oscillator, we derive the Hamiltonian of resonator as the summation of all n terms:

$$\mathcal{H} = \sum_{n=0}^{N-1}\left[\frac{1}{2C_o}Q_n^2 + \frac{1}{2L_o}\left(\Phi_{n+1}^2 - \Phi_n^2\right)\right] \tag{43}$$

The telegrapher model is a discrete representation of the resonator. Thus, by going to the continuum limit, we define:

$$l_o \equiv \frac{L_o}{\Delta x} \qquad c_o \equiv \frac{C_o}{\Delta x}$$

Where l_o and c_o are the inductance per unit length and the capacitance per unit length, respectively. The flux Φ_n is no longer discrete, it becomes a function of position: $\Phi_n = \Phi(x_n)$. And the charge Q_n is described as $Q_n = Q'(x_n)\Delta x$, where $Q'(x_n)$ is the charge density as a function of position.

Hence, the Hamiltonian in continuum limit would be:

$$\mathcal{H} = \sum_{n=0}^{N-1}\left[\frac{\left(Q'(x_n)\Delta x\right)^2}{2c_o\Delta x} + \frac{\left(\Phi(x_{n+1}) - \Phi(x_n)\right)^2}{2l_o\Delta x}\right] \tag{44}$$

In the limit of Δx is infinitesimally small. Then, Δx is replaced by dx, so the Hamiltonian becomes:

$$\mathcal{H} = \int_0^d \underbrace{\left[\frac{c_o}{2}\left(\frac{\partial\Phi}{\partial t}\right)^2 + \frac{1}{2l_o}\left(\frac{\partial\Phi}{\partial x}\right)^2\right]}_{\mathcal{H}_D} dx \tag{45}$$

Where we have used:

$$\frac{\partial\Phi}{\partial x} = \lim_{\Delta x \to 0}\left(\frac{\Phi(x_{n+1}) - \Phi(x_n)}{\Delta x}\right)$$

The integrand in (45), is called the *Hamiltonian density*, $\mathcal{H}_D$ [25]. Because the flux coordinate variable Φ and the momentum *density* conjugate $Q' = c_o\frac{\partial\Phi}{\partial t}$ are field operators inside the waveguide.

The next step is to integrate the Hamiltonian density. This cannot be done unless the field flux variable is derived from the Hamiltonian density. For further details, see Appendix C. Then, the Hamiltonian of the resonator is:

$$\mathcal{H} = \sum_{m=0}^{\infty}\left[\frac{Q_m^2}{2C_r} + \frac{1}{2}C_r\omega_m^2\Phi_m^2\right] \tag{46}$$

Where $C_r = c_o d$ is the total capacitance of the transmission line resonator. This is the classical Hamiltonian of the resonator including all the modes (frequencies) of the resonator. Unlike the LC oscillator, which contains only a single mode. The next step is to quantize the Hamiltonian.

1) Quantization of Transmission Line Resonator: Similar to the LC oscillator discussed in section III, here we have a summation of LC oscillators with different modes. And each mode has it's own operators, so their canonical quantization is $\left[\hat{\Phi}_m, \hat{Q}_{m'}\right] = i\hbar\delta_{mm'}$. Where $\delta_{mm'}$ is a Kronecker delta.

[9]From now, when resonator is mentioned, it means the coplanar waveguide resonator.

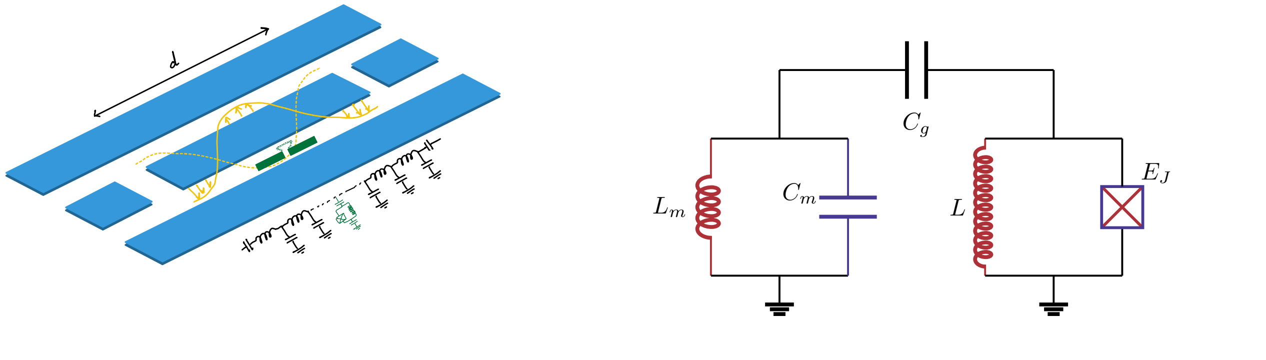

(a) A schematic of fluxonium qubit coupled to a transmission line resonator

(b) Single-mode approximation of fluxonium coupled to resonator

Fig. 12: Coupling Fluxonium qubit to a coplanar waveguide resonator.

Similarly the ladder operators for each mode m are defined as:

$$\hat{\Phi}_m = \sqrt{\frac{\hbar}{2C_r\omega_m}} \left(\hat{a}_m^\dagger + \hat{a}_m\right) \tag{47}$$

$$\hat{Q}_m = i\sqrt{\frac{\hbar C_r \omega_m}{2}} \left(\hat{a}_m^\dagger - \hat{a}_m\right) \tag{48}$$

Where C_r is the resonator's capacitance and ω_m is the mode frequency. And $\hat{a}_m^\dagger$ and $\hat{a}_m$ are the creation and annihilation operators for mode m, respectively. Thus, the Hamiltonian in ladder operators will be:

$$\hat{\mathcal{H}}_{Resonator} = \sum_{m=0}^{\infty} \hbar\omega_m \left(\hat{a}_m^\dagger \hat{a}_m + \frac{1}{2}\right) \tag{49}$$

In other words, the resonator is the sum of infinite quantum harmonic oscillators of different modes.

2) Interaction Hamiltonian: To find the interaction Hamiltonian, we just need to sum both Hamiltonians:

$$\hat{\mathcal{H}} = \hat{\mathcal{H}}_{Fluxonium} + \hat{\mathcal{H}}_{Resonator}$$

Then, we have:

$$\begin{aligned} \hat{\mathcal{H}} = 4E_C\hat{n}^2 + \frac{1}{2}E_L\hat{\varphi}^2 - E_J\cos\left(\hat{\varphi} - \hat{\varphi}_r\right) \\ + \sum_{m=0}^{\infty} \hbar\omega_m \left(\hat{a}_m^\dagger \hat{a}_m + \frac{1}{2}\right) \end{aligned} \tag{50}$$

Here $\hat{\varphi}_r$ is not the offset phase as previously, because now it is coupled to the transmission line. It is rather a continuous flux offset regarding the coupling. By writing the Hamiltonian in ladder operators and doing the single-mode approximation:

$$\begin{aligned} \hat{\mathcal{H}} = \sqrt{8E_C E_L}\left(\hat{b}^\dagger\hat{b} + \frac{1}{2}\right) - E_J\cos\left(\hat{\varphi} - \varphi_r\right) \\ + \hbar\omega_m \left(\hat{a}_m^\dagger \hat{a}_m + \frac{1}{2}\right) \end{aligned} \tag{51}$$

By writing the cosine term in exponential form, it is:

$$-E_J\cos\left(\hat{\varphi} - \varphi_r\right) = -\frac{E_J}{2}\left(exp(i(\hat{\varphi} - \varphi_r)) + H.c.\right)$$

Where H.c. means Hermitian conjugate. In order to find the operator $\hat{\varphi}_r$ we should analyze the fluxonium qubit coupled to an LC oscillator (because here we applied the single-mode approximation), see Fig. 12b.

There is a whole journey after coupling the qubit with a resonator. The next step includes measuring the qubit state and identify the error in signal and so on. This part is not covered in this article. These are suggested for further reading [17, 26].

VI. Applications

The superconducting qubits could be applied for different purposes. The main application and motivation for improving the superconducting qubits is quantum computing, which is discussed in the first subsection. In addition to quantum computing, other applications of superconducting qubits are discussed briefly in the second subsection.

A. Quantum computing

The ultimate goal of the field of quantum computing is to make a reliable quantum computer that can do important computational tasks that cannot be achieved by classical computers or supercomputers. In this section, we discuss some related topics to quantum computing.

1) DiVincenzo Criteria: After discussing the superconducting qubits and briefly reviewing other physical qubits in sections I and II, how could we have a quantum computer with these qubits? To answer this, there is a set of physical requirements to implement a quantum computer[10], known as *DiVincenzo criteria* [27]. Here they are:

1) A scalable physical system with well-defined qubits.

[10] This can be applied to all types of qubits; it's not restricted to superconducting qubits.

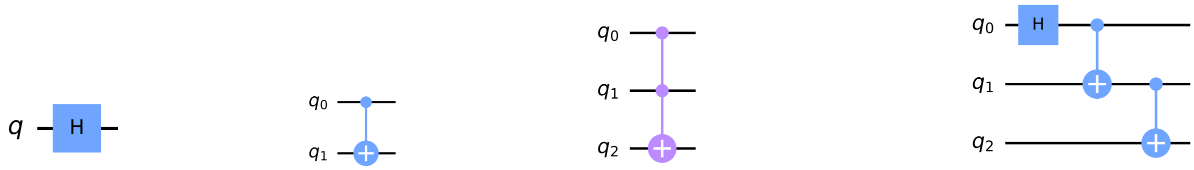

(a) H gate (b) CNOT gate (c) Toffoli gate (d) GHZ

Fig. 13: Quantum circuits: (a) Hadamard gate, (b) CNOT gate, (c) Toffoli gate; is the controlled-controlled-NOT gate and it's a 3-qubit gate and (d) $|GHZ\rangle$ state. The solid dot indicates the controlled qubit and $\oplus$ indicates the target qubit. Also, $\oplus$ means the XOR of the controlled and the target qubit.

2) The ability to initialize the qubit to a specific state.
3) Having a long decoherence time T_2: where T_2 is the dephasing time of the qubit, and it determines the time that we can perform quantum logic gates.
4) A universal set of quantum logical gates.
5) The ability to perform a qubit-specific measurement.

And there are two additional requirements for quantum computers to perform quantum communications: resume

1) The ability to interconvert between stationary qubit and flying qubit.
2) The ability to transmit flying qubits between specified locations.

Flying Qubit: The flying qubits, contrary to stationary qubits, transmit information over macroscopic scales and perform at room temperature. A flying qubit can be achieved by initializing a qubit in such a coherent superposition between the ground and first excited states:

$$|\psi_{initial}\rangle = \alpha|g\rangle + \beta|e\rangle$$

After some time, the qubit will spontaneously decay to the ground state (if it is excited) and into an electromagnetic field in superposition between the photon's states $|0\rangle$ and $|1\rangle$. Then the final state would be a product of the qubit in the ground state and the photon state in superposition inherited from the qubit's initialization:

$$|\psi_{final}\rangle = |g\rangle|\psi_{photon}\rangle = |g\rangle[\alpha|0\rangle + \beta|1\rangle]$$

2) Quantum Gates and Entanglement: Quantum logic gates act on one or more qubits to execute quantum computation. They are the quantum version of classical logic gates, discussed in section I. But not all quantum gates are the quantum version of classical logic gates because qubits have intrinsic properties that are exploited in computations that classical bits don't have.

Here are some of these quantum gates: Pauli *X* gate (or the quantum version of classical NOT gate), Pauli *Y* gate, Pauli *Z* gate, phase gate (*S*), Hadamard (*H*), controlled-NOT gate (CNOT or C*X*), SWAP gate, Toffoli gate, etc. Here we are interested in both Hadamard gate and controlled-NOT gate to show how to perform a maximally 3-qubit entangled state.

Let's give a brief description of *H* and CNOT gates:

- **Hadamard (*H*):**
It is a single-qubit gate, which acts on one qubit only. It turns state $|0\rangle$ into $|+\rangle$ and $|1\rangle$ into $|-\rangle$, i.e.

$$H|0\rangle = \frac{1}{\sqrt{2}}(|0\rangle + |1\rangle) \equiv |+\rangle$$

$$H|1\rangle = \frac{1}{\sqrt{2}}(|0\rangle - |1\rangle) \equiv |-\rangle$$

- **Controlled-NOT (CNOT):**
It is, in contrast to Hadamard gate, a two-qubit gate. It acts on the product state of two qubits by inverting the right qubit, called *target qubit*, if the left qubit, called *controlled qubit*, is in state $|1\rangle$. That is:

$$CNOT|00\rangle = |00\rangle$$

$$CNOT|01\rangle = |01\rangle$$

$$CNOT|10\rangle = |11\rangle$$

$$CNOT|11\rangle = |10\rangle$$

This gate inverts the target qubit, which is performing *X* gate on the right qubit, that is why it's called controlled-NOT gate or controlled-*X* gate (C*X*). The output of CNOT gate has the left qubit the same as the controlled qubit, while the right qubit becomes the XOR of the inputs (the controlled and target qubits), see Fig. 1a. Then we can say that CNOT is the quantum version of classical XOR gate.

Fig. 13a and 13b shows the Hadamard and CNOT gates in quantum circuits by using Qiskit software [28].

The maximally entangled 3-qubit state can be obtained using two different ways:

$$|GHZ\rangle = \frac{1}{\sqrt{2}}(|000\rangle + |111\rangle)$$

Or

$$|W\rangle = \frac{1}{\sqrt{3}}(|001\rangle + |010\rangle + |001\rangle)$$

Here we are going to discuss the process of having $|GHZ\rangle$ state by using Hadamard and CNOT gates [29]. The $|GHZ\rangle$ protocol starts by initializing the three qubits at the ground state, i.e. $|000\rangle$. Then applying Hadamard gate on the first qubit (q_0), i.e.

$$H|000\rangle = \frac{1}{\sqrt{2}}(|000\rangle + |100\rangle)$$

Note that the second (q_1) and third (q_2) qubits remain in the ground state. After that applying the CNOT gate on q_1 conditioned on q_0:

$$CNOT\frac{1}{\sqrt{2}}(|000\rangle + |100\rangle) = \frac{1}{\sqrt{2}}(|000\rangle + |110\rangle)$$

By applying CNOT again on q_2 conditioned on q_1:

$$CNOT\frac{1}{\sqrt{2}}(|000\rangle + |110\rangle) = \frac{1}{\sqrt{2}}(|000\rangle + |111\rangle)$$

Thus, we have $|GHZ\rangle$ state by using Hadamard and CNOT gates. Fig. 13d (as depicted on the previous page) shows the quantum circuit for implementing this state.

There is another way to perform the $|GHZ\rangle$ state by using iSWAP gate discussed in [29]. This is the abstract way to have maximally entangled 3-qubit states, but we did not discuss the practical way to do it, to witness it and confirm the entanglement. In [29], superconducting phase qubits are used for this purpose.

3) Quantum Measurement: The measurement process of the qubit's state is not an easy task. Because the measurement device can influence the qubit to be coupled with it and hence give false results. The measurement process in circuit QED requires a more thorough and detailed investigation, which is not tackled here in this article.

However, quantum measurements are important and give another advantage to quantum computation. Well, the way discussed above to perform computation is based on quantum gate operations, which is called the *quantum circuit model*; it is the quantum version of classical computation. In essence, quantum measurements offer the so-called measurement-based quantum computation (MBQC) [30].

B. Other applications

The applications of superconducting qubits are not focused solely on quantum computing and quantum information processing applications. The flexibility in manipulating the energy states of superconducting qubits enables us to explore novel quantum systems. Due to this, there are several applications of superconducting qubits in the fundamentals of physics and in different physical applications. Here are some of these applications:

Quantum machines: In 2010, the first quantum machine was made by coupling a mechanical resonator and a phase qubit. The importance of quantum machine is to be used in quantum detectors and to generate quantum states of light [31, 32].

Single qubit lasing: Since superconducting qubits are considered as artificial atoms because their energy levels are highly controllable and easy to manipulate. This allows us to explore further quantum-optics phenomena such as lasing using superconducting qubits [33, 34].

Quantum transistor: Classical transistors are the building units of all current technological devices. Generally, classical transistors work by either passing or blocking the coming current. Similarly, quantum transistors change the spin state. In [35], four transmon qubits were used to make a quantum transistor.

Quantum diode: The phenomenon of preferred direction of flow in semiconductors was utilized to make the diode. However, a similar effect occurs in superconducting materials. Implementing superconducting qubits to make real superconducting quantum diodes was examined in [36, 37].

Metamaterials: The materials that are engineered and synthesized to have properties are rarely seen in nature are called *metamaterials*. Such materials, have numerous applications in many fields. Superconducting qubits can be used to construct metamaterials [14].

And many other applications such as the quantum refrigerator [38], which investigates the relationship between quantum mechanics and thermodynamics. In addition to demonstrating Berry's phase [39] and simulating quantum systems [40].

VII. Conclusion

In conclusion, quantum computing will play a crucial role in framing the upcoming technology and pushing the boundaries of the current knowledge. In this article, the definition of qubit was revised in details. A brief discussion on the physical realization of qubits. Followed by a thorough derivation of the mathematical tools and physical models for studying superconducting qubits. In section IV, the different designs of superconducting qubits were reviewed. Circuit QED was established in section V and fluxonium qubit was coupled to a coplanar waveguide resonator. Lastly, in section VI, the applications of superconducting qubits in computation and information processing were reviewed, and briefly, the applications in scientific field.

Appendix A: Superconductivity

In this appendix, we give a brief introduction to superconductors and their main properties, in addition to explaining Josephson's effects. This appendix is based on [41, 42].

A. Electromagnetic View of Superconductivity

1) Zero Resistance: The zero resistance of the superconductor makes it a dissipation-less medium. In other words, there is no damping or loss of energy. This is a common property between the perfect conductor and the superconductor.

2) Meissner-Ochsenfeld Effect: It is the ability of the superconductor to expel the magnetic field outside it. In contrast to the zero resistance, this property is unique to superconductors since they maintain a zero magnetic field inside them. This is the main difference between normal conductors and superconductors.

B. Solid-state View of Superconductivity

In a solid-state view of superconductivity, when specific conductors are cooled to very low temperatures, called the *critical temperature* T_C, below which the free electrons are coming together into pairs, these pairs of electrons are called *Cooper pairs*. Even though we do not know the mechanics of pairing, we know that they are there.

Also, if you have a ring of a superconductor, then the magnetic flux through this ring is quantized! The single quantity of magnetic flux is called *fluxon* ϕ_0 and equals to $h/2e$, where h is Planck's constant, and e is the electron's charge. The fluxon shows that the fundamental charge in a superconductor is $2e$, so it proves the existence of Cooper pairs.

C. Josephson Effects

The Josephson junction consists of two superconductors separated by a thin insulator layer (SIS) or by a non-superconducting layer (SNS). The Josephson junction shows two main effects that have important roles and are exploited by superconducting qubits.

1) DC Josephson Effect: It says: a DC current flows across the Josephson junction in the absence of the electric or magnetic field. This current is given by:

$$I = I_c \sin(\varphi_L - \varphi_R) \tag{52}$$

Where I_c is the critical current and it's proportional to the tunneling rate of Cooper pairs through the junction, $(\varphi_L - \varphi_R)$ is the phase difference through the junction's left and right sides.

2) AC Josephson Effect: If there is a voltage applied to the junction, then the current oscillates with time. That is because the phase difference, i.e. $\varphi_L - \varphi_R$, is now depending on time and proportional to the applied voltage by this relation:

$$\frac{\partial(\varphi_L - \varphi_R)}{\partial t} = -\frac{2eV}{\hbar} \tag{53}$$

Then the oscillating current is:

$$I = I_c \sin\left(\varphi_L - \varphi_R - 2eVt/\hbar\right) \tag{54}$$

So now the current is not constant, but also changes periodically with time in a the effect of the applied voltage.

Appendix B: Lagrangian Formalism and Kirchhoff's Rules

To show that Lagrangian formalism gives the same results as Kirchhoff's rules, we have to derive the equation of motion by both methods and show that they are the same. The equation of motion, in our case for electrical circuits, is how the current[11] changes with time. In our example circuit, the LC oscillator, the equation of motion is how the current changes with time between the elements of inductance L and capacitance C. Note that there are no resistive elements in the example circuit, since superconductors have zero resistance, see Appendix A.

[11]It is not restricted on how current changes with time, but any dynamical variable in the circuit since they are all related. You can rewrite the equation of motion in terms of charge or flux.

A. Lagrangian Formalism

Starting with Lagrangian formalism, to derive the equation of motion of the current, we need to invoke Euler-Lagrange equation for the dynamical operator Q:

$$\frac{d}{dt}\left(\frac{\partial \mathcal{L}}{\partial \dot{Q}}\right) = \frac{\partial \mathcal{L}}{\partial Q} \tag{55}$$

Substituting the Lagrangian of the LC oscillator (10), into the above equation. Then the equation of motion is:

$$\ddot{Q} = -\frac{1}{LC} Q \tag{56}$$

Similarly for the flux dynamical variable Φ, the corresponding Euler-Lagrange equation is:

$$\frac{d}{dt}\left(\frac{\partial \mathcal{L}}{\partial \dot{\Phi}}\right) = \frac{\partial \mathcal{L}}{\partial \Phi} \tag{57}$$

Substituting the Lagrangian in the above equation, getting the equation of motion for Φ:

$$\ddot{\Phi} = -\frac{1}{LC} \Phi \tag{58}$$

As we will show later, solving (58) and (56) would give us the same equations of motion as Kirchhoff's rules.

B. Kirchhoff's Rules

In Kirchhoff's rules, we start with associating a charge branch and a flux branch which are defined here as in [43, 44]:

$$\Phi_i(t) = \int_{-\infty}^{t} V_i(t')dt' \tag{59}$$

$$Q_i(t) = \int_{-\infty}^{t} I_i(t')dt' \tag{60}$$

where $i = A, B$ are the branches of the circuit shown in Fig. 2. Alternatively, it is better to write (59) and (60) as: $V_i = \dot{\Phi}_i$ and $I_i = \dot{Q}_i$ for each branch. We are dealing with Kirchhoff's rules (i.e. we are dealing with voltages and currents).

Now, by voltage rule: $V_A + V_B = 0$, and the associated branch fluxes we get[12]:

$$\begin{aligned} &-\dot{\Phi}_A + \dot{\Phi}_B = 0 \\ &\Rightarrow -L\dot{I}_A = \dot{\Phi}_B \end{aligned} \tag{61}$$

Differentiating (61) with respect to time:

$$-L\ddot{I}_A = \ddot{\Phi}_B \tag{62}$$

Note that there is only one independent variable because Kirchhoff's rules constrain the degrees of freedom. From current law $I_A + I_B = 0$ we get:

$$I_A + C\ddot{\Phi}_B = 0 \tag{63}$$

Here $I_B = \dot{Q}_B = \frac{d}{dt}(C\dot{\Phi}_B) = C\ddot{\Phi}_B$. Then,

$$\ddot{\Phi}_B = -\frac{I_A}{C} \tag{64}$$

[12]The sign of fluxes are arbitrary chosen, you can change the sign convention and you wold get the same result.

Substituting (64) into (62):

$$-L\ddot{I}_A - \frac{I_A}{C} = 0$$

$$\Rightarrow \ddot{I}_A = -\frac{1}{LC} I_A \tag{65}$$

Here (65) will have the same solution as (56) and (58). Let's solve the above equation (65):

$$I_A(t) = I_{A_{max}} \cos(\omega t + \delta) \tag{66}$$

where $\omega = 1/\sqrt{LC}$ and $I_{A_{max}}$ and δ can be determined by the initial conditions. Equation (66) can be written in terms of Φ_A or Q_A, since we know their relation together.

APPENDIX C: SOLVING RESONATOR'S HAMILTONIAN

In order to find the Hamiltonian of the resonator, we need to use the Hamiltonian field theory. This starts by deriving the field flux variable Φ from the density Hamiltonian in (45).

To find the equation of motion, from which we can find the field flux by solving it, we first need the Hamiltonian field equations which they are [45]:

$$\dot{\phi} = \frac{\delta \mathcal{H}_D}{\delta \pi} \tag{67}$$

$$\dot{\pi} = -\frac{\delta \mathcal{H}_D}{\delta \phi} \tag{68}$$

Where ϕ is the field and π is the momentum density conjugate to the field. Here $\frac{\delta}{\delta f}$ is the variational derivative defined as:

$$\frac{\delta}{\delta f} = \frac{\partial}{\partial f} - \nabla \cdot \frac{\partial}{\partial(\nabla f)} \tag{69}$$

Since we have only 1 spatial dimension, x-axis along the length of the resonator, then the variational derivative is:

$$\frac{\delta}{\delta f} = \frac{\partial}{\partial f} - \frac{\partial}{\partial x}\left(\frac{\partial}{\partial(\frac{\partial f}{\partial x})}\right) \tag{70}$$

By using the second Hamiltonian equation (68), on the Hamiltonian density $\mathcal{H}_D$:

$$\dot{\pi} = \frac{\partial \mathcal{H}_D}{\partial \Phi} - \frac{\partial}{\partial x}\left(\frac{\partial \mathcal{H}_D}{\partial(\frac{\partial \Phi}{\partial x})}\right)$$

We have:

$$c_o \frac{\partial^2 \Phi}{\partial t^2} = -\frac{\partial}{\partial \Phi}\left(\frac{c_o}{2}\left(\frac{\partial \Phi}{\partial t}\right)^2 + \frac{1}{2l_o}\left(\frac{\partial \Phi}{\partial x}\right)^2\right) + \frac{\partial}{\partial x}\left(\frac{1}{l_o}\frac{\partial \Phi}{\partial x}\right)$$

Then:

$$c_o \frac{\partial^2 \Phi}{\partial t^2} = -\left(\frac{c_o}{2}\frac{\partial^2 \Phi}{\partial t^2} + \frac{1}{2l_o}\frac{\partial^2 \Phi}{\partial x^2}\right) + \frac{1}{l_o}\frac{\partial^2 \Phi}{\partial x^2}$$

After simplification, we got the equation of motion:

$$\frac{\partial^2 \Phi}{\partial t^2} = v_o^2 \frac{\partial^2 \Phi}{\partial x^2} \tag{71}$$

This is the wave equation, where $v_o^2 = 1/c_o l_o$. The solution of the wave equation by using separation of variable method[13] for one mode:

$$\Phi(x,t) = \sum_{m=0}^{\infty} u_m(x)\Phi_m(t) \tag{72}$$

Substituting into wave equation (71):

$$\frac{\partial^2}{\partial t^2}\left(u_m(x)\Phi_m(t)\right) = {v_o}^2 \frac{\partial^2}{\partial x^2}\left(u_m(x)\Phi_m(t)\right)$$

Then,

$$\frac{1}{\Phi_m}\frac{d^2\Phi_m}{dt^2} = {v_o}^2 \frac{1}{u_m}\frac{d^2 u_m}{dx^2} = -\omega_m^2$$

The first equality (temporal part) is $\ddot{\Phi}_m = -\omega_m^2 \Phi_m$, and it is arbitrary (i.e. not necessarily a sinusoidal). That is because we do not have boundary conditions on time. The second equality (spatial part) is:

$$\frac{d^2 u_m}{dx^2} = -k_m^2 u_m \tag{73}$$

where $k_m = \omega_m / v_o$. Hence the solution of the spatial part is:

$$u_m(x) = A_m \cos(k_m x + \delta_m) \tag{74}$$

The boundary conditions (for $\lambda/2$ coplanar waveguide resonator) are:

$$I(x = 0, d) = -\frac{1}{l_o}\frac{\partial \Phi}{\partial x}\bigg|_{x=0,d} = 0 \tag{75}$$

Applying the boundary conditions on the spatial part, which is (74). With simple substitution, we get $\delta_m = 0$ and $k_m = \frac{m\pi}{d}$. Then, the solution of the spatial part of the wave equation is:

$$u_m(x) = A_m \cos(\frac{m\pi}{d} x) \tag{76}$$

Then summing over all modes, the general solution is:

$$\begin{aligned}\Phi(x,t) &= \sum_{m=0}^{\infty} u_m(x)\Phi_m(t) \\ &= \sum_{m=0}^{\infty} A_m \cos(\frac{m\pi}{d} x)\Phi_m(t)\end{aligned} \tag{77}$$

Exploiting the orthogonality of the different modes, we have the normalization rules[14] for the spatial solution:

$$\frac{1}{d}\int_0^d u_m u_{m'}\, dx = \delta_{mm'} \tag{78}$$

$$\frac{1}{k_m^2 d}\int_0^d \frac{\partial u_m}{\partial x}\frac{\partial u_{m'}}{\partial x}\, dx = \delta_{mm'} \tag{79}$$

Substitute back in the Hamiltonian density (45), with:

$$\frac{\partial \Phi}{\partial t} = \sum_{m=0}^{\infty} u_m(x)\frac{\partial \Phi_m}{\partial t} \tag{80}$$

[13]Notice that $u_m(x)$ is a dimensionless function.

[14]These normalization rules keep the spatial part $u_m(x)$ dimensionless.

$$\frac{\partial \Phi}{\partial x} = \sum_{m=0}^{\infty} \frac{\partial u_m}{\partial x} \Phi_m \tag{81}$$

Thus:

$$\mathcal{H} = \int_0^d \left[\frac{c_o}{2} \sum_{m=0}^{\infty} \sum_{m'=0}^{\infty} u_m(x) u_{m'}(x) \frac{\partial \Phi_m}{\partial t} \frac{\partial \Phi_{m'}}{\partial t} + \frac{1}{2l_o} \sum_{m=0}^{\infty} \sum_{m'=0}^{\infty} \frac{\partial u_m}{\partial x} \frac{\partial u_{m'}}{\partial x} \Phi_m \Phi_{m'} \right] dx \tag{82}$$

By applying the normalization rules:

$$\mathcal{H} = \frac{c_o d}{2} \sum_{m=0}^{\infty} \left(\frac{\partial \Phi_m}{\partial t} \right)^2 + \frac{d}{2l_o} \sum_{m=0}^{\infty} k_m^2 \Phi_m^2 \tag{83}$$

Simplifying the expression and taking a common factor:

$$\mathcal{H} = \frac{c_o d}{2} \sum_{m=0}^{\infty} \left[\left(\frac{\partial \Phi_m}{\partial t} \right)^2 + \omega_m^2 \Phi_m^2 \right] \tag{84}$$

Substituting back with charge density $Q'_m = c_o \frac{\partial \Phi_m}{\partial t}$:

$$\mathcal{H} = \frac{c_o d}{2} \sum_{m=0}^{\infty} \left[\frac{1}{c_o^2} {Q'_m}^2 + \omega_m^2 \Phi_m^2 \right] \tag{85}$$

The charge for mode m is $Q_m = Q'_m d$, substituting this back, we get:

$$\mathcal{H} = \sum_{m=0}^{\infty} \left[\frac{Q_m^2}{2C_r} + \frac{1}{2} C_r \omega_m^2 \Phi_m^2 \right] \tag{86}$$

Where $C_r = c_o d$ is the total capacitance of the transmission line resonator. And, finally, we have the classical Hamiltonian of the transmission line resonator.

Acknowledgment

The authors thank the financial support from the University of Bahrain.

References

[1] David Deutsch. “Quantum theory, the Church–Turing principle and the universal quantum computer”. In: *Proceedings of the Royal Society of London A Mathematical and Physical Sciences* 400.1818 (July 1985), pp. 97–117. DOI: 10.1098/rspa.1985.0070. URL: https://doi.org/10.1098/rspa.1985.0070.

[2] Peter W Shor. “Algorithms for quantum computation: discrete logarithms and factoring”. In: *Proceedings 35th annual symposium on foundations of computer science*. Ieee. 1994, pp. 124–134.

[3] Peter W Shor. “Polynomial-time algorithms for prime factorization and discrete logarithms on a quantum computer”. In: *arXiv [quant-ph]* (1995).

[4] Lov K Grover. “A fast quantum mechanical algorithm for database search”. In: *Proceedings of the twenty-eighth annual ACM symposium on Theory of computing - STOC ’96*. Philadelphia, Pennsylvania, United States: ACM Press, 1996.

[5] Iulia Georgescu. “A bit on the bit”. In: *Nature Physics* 12.9 (2016), pp. 888–888. ISSN: 1745-2481. DOI: 10.1038/nphys3878. URL: https://doi.org/10.1038/nphys3878.

[6] Niklas Mueller et al. “Quantum computation of dynamical quantum phase transitions and entanglement tomography in a lattice gauge theory”. en. In: *PRX quantum* 4.3 (Aug. 2023).

[7] Matt Swayne. *Intel Chips Away at Fault-Tolerant Quantum Computing With Latest Advance — thequantuminsider.com*. https://thequantuminsider.com/2024/05/02/intel-chips-away-at-fault-tolerant-quantum-computing-with-latest-cryogenic-advance/. [Accessed 22-02-2025].

[8] William J Gallagher, Erik P Harris, and Mark B Ketchen. “Superconductivity at IBM–a centennial review: part I–superconducting computer and device applications”. In: *Proceedings of the IEEE/CSC ESAS European Superconductivity News Forum*. Vol. 21. 2012, pp. 1–34.

[9] Rachel Courtland. “Google aims for quantum computing supremacy [news]”. In: *IEEE Spectrum* 54.6 (2017), pp. 9–10.

[10] *Amazon Braket launches new superconducting quantum processor from IQM — Amazon Web Services — aws.amazon.com*. https://aws.amazon.com/blogs/quantum-computing/amazon-braket-launches-new-superconducting-quantum-processor-from-iqm/. [Accessed 22-02-2025].

[11] Galan Moody et al. “2022 Roadmap on integrated quantum photonics”. In: *Journal of Physics: Photonics* 4.1 (2022), p. 012501. DOI: 10.1088/2515-7647/ac1ef4. URL: https://dx.doi.org/10.1088/2515-7647/ac1ef4.

[12] Herbert Goldstein, Charles P Poole, and John L Safko. *Classical Mechanics*. 3rd ed. Upper Saddle River, NJ: Pearson, June 2001.

[13] David J Griffiths and Darrell F Schroeter. *Introduction to Quantum Mechanics*. 3rd ed. Cambridge, England: Cambridge University Press, Aug. 2018.

[14] Xiu Gu et al. “Microwave photonics with superconducting quantum circuits”. In: *Physics Reports* 718-719 (2017), pp. 1–102. ISSN: 0370-1573. DOI: https://doi.org/10.1016/j.physrep.2017.10.002.

[15] Morten Kjaergaard et al. “Superconducting qubits: Current state of play”. en. In: *Annu. Rev. Condens. Matter Phys.* 11.1 (Mar. 2020), pp. 369–395.

[16] Jens Koch et al. “Charge-insensitive qubit design derived from the Cooper pair box”. In: *Physical Review A* 76.4 (2007), p. 042319.

[17] Alexandre Blais et al. “Circuit quantum electrodynamics”. In: *Reviews of Modern Physics* 93.2 (2021), p. 025005.

[18] Eric Hyyppä et al. “Unimon qubit”. In: *Nature Communications* 13.1 (2022), p. 6895.

[19] WC Smith et al. "Superconducting circuit protected by two-Cooper-pair tunneling". In: *npj Quantum Information* 6.1 (2020), p. 8.
[20] Ivan V Pechenezhskiy et al. "The superconducting quasicharge qubit". In: *Nature* 585.7825 (2020), pp. 368–371.
[21] Konstantin Kalashnikov et al. "Bifluxon: Fluxon-parity-protected superconducting qubit". In: *PRX Quantum* 1.1 (2020), p. 010307.
[22] Feng-Ming Liu et al. "Quantum design for advanced qubits: plasmonium". In: *arXiv preprint arXiv:2109.00994* (2021).
[23] P Krantz et al. "A quantum engineer's guide to superconducting qubits". en. In: *Appl. Phys. Rev.* 6.2 (June 2019), p. 021318.
[24] David M Pozar. *Microwave Engineering*. en. 4th ed. Chichester, England: John Wiley & Sons, Nov. 2011.
[25] Michael E Peskin and Daniel V Schroeder. *An introduction to quantum field theory an introduction to quantum field theory*. London, England: CRC Press, Sept. 2019.
[26] A A Clerk et al. "Introduction to quantum noise, measurement, and amplification". en. In: *Rev. Mod. Phys.* 82.2 (Apr. 2010), pp. 1155–1208.
[27] David P DiVincenzo. "The physical implementation of quantum computation". In: *Fortschritte der Physik: Progress of Physics* 48.9-11 (2000), pp. 771–783.
[28] Qiskit contributors. *Qiskit: An Open-source Framework for Quantum Computing*. 2023. DOI: 10.5281/zenodo.2573505.
[29] Matthew Neeley et al. "Generation of three-qubit entangled states using superconducting phase qubits". In: *Nature* 467.7315 (2010), pp. 570–573.
[30] Hans J Briegel et al. "Measurement-based quantum computation". In: *Nature Physics* 5.1 (2009), pp. 19–26.
[31] Adrian Cho. "The First Quantum Machine". In: *Science* 330.6011 (2010), pp. 1604–1604. DOI: 10.1126/science.330.6011.1604.
[32] A D O'Connell et al. "Quantum ground state and single-phonon control of a mechanical resonator". en. In: *Nature* 464.7289 (Apr. 2010), pp. 697–703.
[33] O Astafiev et al. "Single artificial-atom lasing". In: *Nature* 449.7162 (2007), pp. 588–590.
[34] S Ashhab et al. "Single-artificial-atom lasing using a voltage-biased superconducting charge qubit". In: *New J. Phys.* 11.2 (Feb. 2009), p. 023030.
[35] Niels Jakob Søe Loft et al. "Quantum spin transistors in superconducting circuits". In: *arXiv preprint arXiv:1802.04292* (2018).
[36] Rishabh Upadhyay et al. "Microwave quantum diode". In: *arXiv preprint arXiv:2304.00799* (2023).
[37] Xuedong Zhao et al. "Engineering quantum diode in one-dimensional time-varying superconducting circuits". In: *npj Quantum Information* 9.1 (2023), p. 59.
[38] Andrew Guthrie et al. "Cooper-Pair Box Coupled to Two Resonators: An Architecture for a Quantum Refrigerator". In: *Physical Review Applied* 17.6 (2022). DOI: 10.1103/physrevapplied.17.064022. URL: https://doi.org/10.1103%2Fphysrevapplied.17.064022.
[39] Peter J Leek et al. "Observation of Berry's phase in a solid-state qubit". In: *science* 318.5858 (2007), pp. 1889–1892.
[40] Göran Wendin. "Quantum information processing with superconducting circuits: a review". In: *Reports on Progress in Physics* 80.10 (2017), p. 106001.
[41] Charles Kittel. *Introduction to solid state physics*. en. 8th ed. Nashville, TN: John Wiley & Sons, Oct. 2004.
[42] James F Annett. *Superconductivity, Superfluids and Condensates*. en. Oxford Master Series in Physics. London, England: Oxford University Press, Mar. 2004.
[43] Uri Vool and Michel Devoret. "Introduction to quantum electromagnetic circuits". In: *International Journal of Circuit Theory and Applications* 45.7 (2017), pp. 897–934.
[44] Jascha Ulrich and Fabian Hassler. "Dual approach to circuit quantization using loop charges". In: *Physical Review B* 94.9 (2016), p. 094505.
[45] Alex Nelson. *Classical Hamiltonian Field Theory*. Available at https://pqnelson.github.io/notebk/hamiltonianFieldTheory.pdf (2023/5/26)).